

Mixing Patterns of Several Kinds of Impellers in Rectangular Vessels

Haruki FURUKAWA, Yoshihito KATO, Yoshitaka FUKATSU, Ryo NAGUMO
and Yutaka TADA

Department of Life and Materials Engineering, Nagoya Institute of Technology,
Gokiso-cho, Showa -ku, Nagoya-shi, Aichi 466-8555, Japan

Keywords: Mixing, Agitation, Mixing Pattern, Rectangular Vessel, Eccentric Mixing

Power numbers of several kinds of impellers in rectangular eccentric vessels were correlated with the modified equation of Kamei *et al.* for a wide range of Reynolds numbers. Mixing patterns of these impellers in rectangular eccentric vessels were also observed for a wide range of Reynolds numbers by using a decolorization method based on the reaction between sodium thiosulfate and iodine. A relationship was established between the power number diagram (N_p-Re diagram) and the shape of the isolated zone. For low Reynolds numbers, isolated zones like doughnut-ring were observed in the rectangular vessels as well as in a cylindrical vessel without baffle.

Introduction

It is well known that an isolated zone (a doughnut-ring-shaped zone in laminar mixing and a cylindrically rotating zone (CRZ) in turbulent mixing) may be generated in an unbaffled vessel when using relatively small impellers such as propeller impellers and turbine impellers (Kato *et al.*, 2010b). The value of Re_d when the doughnut-ring-shaped isolated zone becomes a CRZ has been determined for cylindrical vessels with several kinds of impellers.

Not only a cylinder vessel but a rectangular vessel may be used for an industrial mixing process. Furukawa *et al.* (2013a, 2013b, 2013c) measured the power consumptions of rectangular vessels with several kinds of impellers over a wide range of Reynolds number, from laminar to turbulent flow regions, and correlated them by using the modified versions of Kamei (Kamei *et al.*, 1995, 1996) expressions. The Power number was correlated for a rectangular mixing vessel with a paddle impeller, a pitched paddle impeller, Rushton turbine, and a propeller impeller (2013a, 2013b, 2013c). It was found that the power number of rectangular eccentric mixing vessels corresponded to that of a cylindrical vessel with a diameter of $\sqrt{2}$ times the short side of the horizontal cross section of the rectangular vessel and with one baffle with a width of 1/10 of the rectangular vessel diagonal. In addition, the power numbers of both rectangular and cylindrical eccentric mixing vessels were correlated with the equations of Kamei *et al.* (1995, 1996) by taking the number of baffles as unity and the baffle width as the eccentric length of the mixing shaft.

In this paper, we derive a relationship between the power number diagram and the mixing pattern in rectangular eccentric vessels.

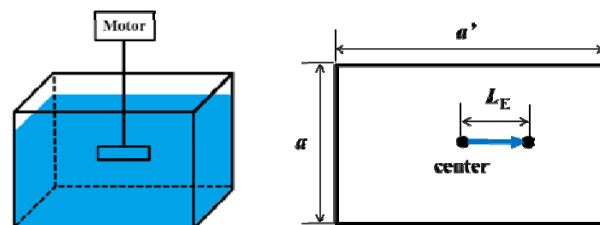


Fig.1 Dimension of rectangular eccentric mixing vessel

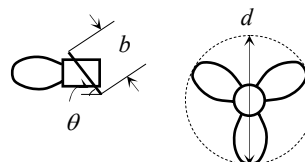


Fig. 2 Dimension of propeller impeller

1. Experimental

The schematic diagram of the rectangular eccentric vessel used in this study is shown in **Figure 1**. The vessel, which was used for measuring power consumption and observing mixing patterns, was rectangular vessel and had a short side (a) of the horizontal cross section of the rectangular vessel of 170 mm. The long side (a') of the horizontal cross section of the rectangular vessel is 255 and 340 mm.

The dimension of propeller impeller is given in **Figure 2**. The geometry of the impellers are shown in **Table 1**. The liquids used for measuring the power consumption and observing the mixing patterns were desalted water and starch syrup solution ($\mu = 0.001 - 5.0$ Pa·s). The vessel was filled with the liquid to a height equal to the characteristic length of $\sqrt{2}$ times the short side (a) of the horizontal cross section of the rectangular

vessel ($H = \sqrt{2}a$). The eccentric length L_E was equal to the $a/4$. The power consumption $P (=2\pi nT)$ was calculated by measuring the shaft torque T and rotational speed n . The mixing pattern was observed by adopting the decolorization method based on the reaction of iodine with sodium thiosulfate in water. The rotational speed n was varied from 60 to 450 rpm. To achieve homogeneous illumination, a sheet of white paper on the rectangular chamber wall was used as a light diffuser. Sodium thiosulfate was added between the impeller and the vessel wall. The mixing pattern was observed and recorded by a CCD camera for 60 min.

Table 1 Geometry of several kinds of impellers

Impeller	d [m]	b [m]	n_p [-]	θ [-]
(1)paddle	0.070	0.028	2	$\pi/2$
(2)paddle	0.076	0.019	6	$\pi/2$
(3)Rushton turbine	0.060	0.012	6	$\pi/2$
(4)pitched paddle	0.070	0.017	6	$\pi/4$
(5)propeller	0.069	0.022	3	$\pi/6$

Table 2 Power number for paddle and Rushton turbine impeller in rectangular vessel

Unbaffled condition

$$N_{P0} = \{[1.2\pi^4\beta^2]/[8d^3/(D^2H)]\}f$$

$$f = C_L/Re_G + C_t\{[(C_{tr}/Re_G) + Re_G]^{-1} + (f_{\infty}/C_t)^{1/m}\}^m$$

$$Re_d = nd^2\rho/\mu$$

$$Re_G = \{\pi\eta\ln(D/d)/(4d/\beta D)\}Re_d$$

$$C_L = 0.215\eta n_p(d/H)[1-(d/D)^2] + 1.83(b/H)(n_p/2)\sin\theta^{1/3}$$

$$C_t = [(1.96X^{1.19})^{-7.8} + (0.25)^{-7.8}]^{-1/7.8}$$

$$m = [(0.71X^{0.373})^{-7.8} + (0.333)^{-7.8}]^{-1/7.8}$$

$$C_{tr} = 23.8(d/D)^{-3.24}(b/D)^{-1.18}X^{0.74}$$

$$f_{\infty} = 0.0151(d/D)C_t^{0.308}$$

$$X = \eta n_p^{0.7}b/H$$

$$\beta = 2\ln(D/d)/[(D/d)-(d/D)]$$

$$\gamma = [\eta\ln(D/d)/(\beta D/d)^5]^{1/3}$$

$$\eta = 0.711\{0.157 + [n_p \ln(D/d)]^{0.611}\}/\{n_p^{0.52}[1-(d/D)^2]\}$$

Center shaft condition

$$N_P = [(1+x^{-3})^{-1/3}]N_{Pmax}$$

$$x = 0.45(\sqrt{a^2 + a'^2}/D)/N_{Pmax}^{0.2} + N_{P0}/N_{Pmax}$$

Eccentric shaft condition

$$N_P = [(1+x^{-3})^{-1/3}]N_{Pmax}$$

$$x = 4.5(L_E/D)/N_{Pmax}^{0.2} + N_{P0}/N_{Pmax}$$

Fully baffled condition

$$N_{Pmax} = 10(n_p^{0.7}b/d)^{1.3} \quad n_p^{0.7}b/d \leq 0.54$$

$$N_{Pmax} = 8.3(n_p^{0.7}b/d) \quad 0.54 < n_p^{0.7}b/d \leq 1.6$$

$$N_{Pmax} = 10(n_p^{0.7}b/d)^{0.6} \quad 1.6 < n_p^{0.7}b/d$$

Table 3 Power number for pitched paddle in rectangular vessel

Unbaffled condition

$$N_{P0} = \{[1.2\pi^4\beta^2]/[8d^3/(D^2H)]\}f$$

$$f = C_L/Re_G + C_t\{[(C_{tr}/Re_G) + Re_G]^{-1} + (f_{\infty}/C_t)^{1/m}\}^m$$

$$Re_d = nd^2\rho/\mu$$

$$Re_G = \{\pi\eta\ln(D/d)/(4d/\beta D)\}Re_d$$

$$C_L = 0.215\eta n_p(d/H)[1-(d/D)^2] + 1.83(b\sin\theta/H)(n_p/2\sin\theta)^{1/3}$$

$$C_t = [(1.96X^{1.19})^{-7.8} + (0.25)^{-7.8}]^{-1/7.8}$$

$$m = [(0.71X^{0.373})^{-7.8} + (0.333)^{-7.8}]^{-1/7.8}$$

$$C_{tr} = 23.8(d/D)^{-3.24}(b\sin\theta/D)^{-1.18}X^{0.74}$$

$$f_{\infty} = 0.0151(d/D)C_t^{0.308}$$

$$X = \eta n_p^{0.7}b\sin^{1.6}\theta/H$$

$$\beta = 2\ln(D/d)/[(D/d)-(d/D)]$$

$$\gamma = [\eta\ln(D/d)/(\beta D/d)^5]^{1/3}$$

$$\eta = 0.711\{0.157 + [n_p \ln(D/d)]^{0.611}\}/\{n_p^{0.52}[1-(d/D)^2]\}$$

Center shaft condition

$$N_P = [(1+x^{-3})^{-1/3}]N_{Pmax}$$

$$x = 0.45(\sqrt{a^2 + a'^2}/D)/\{(2\theta/\pi)^{0.72}N_{Pmax}^{0.2}\} + N_{P0}/N_{Pmax}$$

Eccentric shaft condition

$$N_P = [(1+x^{-3})^{-1/3}]N_{Pmax}$$

$$x = 4.5(L_E/D)/\{(2\theta/\pi)^{0.72}N_{Pmax}^{0.2}\} + N_{P0}/N_{Pmax}$$

Fully baffled condition

$$N_{Pmax} = 8.3(2\theta/\pi)^{0.9}(n_p^{0.7}b\sin^{1.6}\theta/d)$$

Table 4 Power number for propeller in rectangular vessel

Unbaffled condition

$$N_{P0} = \{[1.2\pi^4\beta^2]/[8d^3/(D^2H)]\}f$$

$$f = C_L/Re_G + C_t\{[(C_{tr}/Re_G) + Re_G]^{-1} + (f_{\infty}/C_t)^{1/m}\}^m$$

$$Re_d = nd^2\rho/\mu$$

$$Re_G = \{\pi\eta\ln(D/d)/(4d/\beta D)\}Re_d$$

$$C_L = 0.215\eta n_p(d/H)[1-(d/D)^2] + 1.83(b\sin\theta/H)(n_p/2\sin\theta)^{1/3}$$

$$C_t = [(3X^{1.5})^{-7.8} + (0.25)^{-7.8}]^{-1/7.8}$$

$$m = [(0.8X^{0.373})^{-7.8} + (0.333)^{-7.8}]^{-1/7.8}$$

$$C_{tr} = 23.8(d/D)^{-3.24}(b\sin\theta/D)^{-1.18}X^{0.74}$$

$$f_{\infty} = 0.0151(d/D)C_t^{0.308}$$

$$X = \eta n_p^{0.7}b\sin^{1.6}\theta/H$$

$$\beta = 2\ln(D/d)/[(D/d)-(d/D)]$$

$$\gamma = [\eta\ln(D/d)/(\beta D/d)^5]^{1/3}$$

$$\eta = 0.711\{0.157 + [n_p \ln(D/d)]^{0.611}\}/\{n_p^{0.52}[1-(d/D)^2]\}$$

Center shaft condition

$$N_P = [(1+x^{-3})^{-1/3}]N_{Pmax}$$

$$x = 0.45(\sqrt{a^2 + a'^2}/D)/\{(2\theta/\pi)^{0.72}N_{Pmax}^{0.2}\} + N_{P0}/N_{Pmax}$$

Eccentric shaft condition

$$N_P = [(1+x^{-3})^{-1/3}]N_{Pmax}$$

$$x = 4.5(L_E/D)/\{(2\theta/\pi)^{0.72}N_{Pmax}^{0.2}\} + N_{P0}/N_{Pmax}$$

Fully baffled condition

$$N_{Pmax} = 6.5(n_p^{0.7}b\sin^{1.6}\theta/d)^{1.7}$$

2. Results and Discussion

2.1 Power correlations

The values of the power numbers N_p of paddle impeller and Rushton turbine, pitched paddle and propeller impellers were well correlated with the equations given in **Tables 2, 3** and **Table 4**, respectively. In the center shaft condition, N_{p0} is the power number of a cylindrical mixing vessel with a diameter of $\sqrt{2}$ times the short side of the horizontal cross section of the rectangular vessel without baffle. And in the eccentric shaft condition, N_{p0} is the power number of the rectangular center mixing vessel.

2.2 Mixing Patterns

2.2.1 Paddle impeller

The power consumption and Re_d determined while observing the mixing patterns in the rectangular center mixing and the eccentric mixing vessels with paddle impeller (1) are shown in **Figure 3**. The power number of center mixing vessels (①~④) was the same as that of eccentric mixing vessels (⑤~⑧). **Figure 4** shows the characteristic mixing patterns in the rectangular center mixing vessels (①~④) and the eccentric mixing vessels (⑤~⑧), respectively. These photographs were taken at non-dimensional agitation time $nt = 2000$ where typical mixing patterns were generated. In lower Re_d , an isolated mixing region like doughnut ring was observed in the upper and the lower sides of the impeller in the center shaft mixing, as shown in Fig.4. However, in the eccentric mixing, the isolated mixing region was not observed in more than 15 Reynolds number. At $Re_d = 15$ in the center mixing vessel in Fig. 4, where the power number curve become nearly constant, a pair of doughnut rings was observed, while in the eccentric vessel two smaller doughnut rings rotated with the impeller. For $Re_d > 50$, isolated mixing region was not observed. CRZ was not generated, because a rectangular vessel achieved the same performance as a cylindrical vessel with baffle.

When using paddle impeller (2), the tendency described above was the similar, as shown in **Figures 5** and **6**.

When using the larger rectangular vessel ($a'=340$ mm) with paddle impeller (1), the tendency described above was also the similar, as shown in **Figures 7** and **8**. In addition, in the case of paddle impeller (2), the tendency was the similar, as shown in **Figures 9** and **10**.

2.2.2 Rushton turbine

The power consumption and Re_d determined in the rectangular center mixing vessels (①~④) and the eccentric mixing vessels with Rushton turbine impeller (3) are shown in **Figure 11**. **Figure 12** shows the

characteristic mixing patterns in the rectangular center mixing vessels (①~④) and the eccentric mixing vessels (⑤~⑧), respectively. These photographs were taken at the same non-dimensional agitation time $nt = 2000$ where typical mixing patterns were generated. At $Re_d = 15$ in the center mixing vessel, a pair of doughnut rings was observed, while in the eccentric vessel two smaller doughnut rings rotated with the impeller. The term of “a pair of doughnut rings” indicates “doughnut rings in center mixing”, and the term of “two smaller doughnut rings” indicates “doughnut rings in eccentric mixing”. The authors expressed them like that because the size of doughnut rings in eccentric mixing is smaller than the size of doughnut rings in center mixing. The configuration of the isolated mixing region (IMR) which was tilted against impeller appeared in eccentric mixing vessel. It was considered that the asymmetric flow pattern due to eccentric mixing appeared mainly because Rushton turbine has a disk unlike other impellers. For $Re_d > 50$, isolated mixing region was not observed. CRZ was not generated, because a rectangular vessel achieved the same performance as a cylindrical vessel with baffle.

When using the larger rectangular vessel with Rushton turbine impeller (3), the tendency described above was the similar, as shown in **Figures 13** and **14**.

2.2.3 Pitched paddle impeller

The power consumption and Re_d in the rectangular center mixing vessels (①~④) and the eccentric mixing vessels (⑤~⑧) with pitched paddle impeller (4) are shown in **Figure 15**. **Figure 16** shows the characteristic mixing patterns in the rectangular center mixing vessels (①~④) and the eccentric mixing vessels (⑤~⑧), respectively. These photographs were taken at non-dimensional agitation time $nt = 2000$ where typical mixing patterns were generated. In low $Re_d = 2 - 15$, an isolated mixing region could be observed upper and lower side of the impeller. At $Re_d = 50$ in the center mixing vessel, the doughnut ring under the impeller was larger than that in lower Reynolds number. For $Re_d > 50$, isolated mixing region was not observed. CRZ was not generated, because a rectangular vessel achieved the same performance as a cylindrical vessel with baffle.

When using the larger rectangular vessel with pitched paddle impeller (4), the tendency described above was the similar, as shown in **Figures 17** and **18**.

2.2.4 Propeller impeller

The power consumption and Re_d in the rectangular center mixing vessels (①~④) and the eccentric mixing vessels (⑤~⑧) with propeller impeller (5) are shown in **Figure 19**. **Figure 20** shows the characteristic mixing patterns in the rectangular center mixing vessels (①~

④) and the eccentric mixing vessels (⑤ ~ ⑧), respectively. These photographs were taken at non-dimensional agitation time $nt = 2000$ where typical mixing patterns were generated. No doughnut rings can be found in Figures 20 at ① and ⑤ at $Re=2$. However, a doughnut ring was observed around the impeller by longer time mixing. Up to $Re_d = 50$ in the center mixing vessel, a pair of doughnut rings was observed, while in the eccentric vessel the doughnut rings was not observed in more than 50 Reynolds number. CRZ was not generated, because a rectangular vessel achieved the same performance as a cylindrical vessel with baffle.

When using a larger rectangular vessel with propeller impeller (5), the tendency described above was the similar, as shown in Figures 21 and 22.

Conclusions

By observing the photographs of the mixing patterns in center and eccentric rectangular mixing vessels observed in this study, the three regions in the power number diagram were determined. As long as smaller impellers are used in rectangular vessel, in the laminar region Re_d is less than 10, the power number is inversely proportional to Re_d , and the isolated mixing region was generated in the rectangular vessel as well as the cylindrical vessel. However, in the turbulent region Re_d is larger than 100, a cylindrical rotating zone was not generated, because a rectangular vessel achieved the same performance as a cylindrical vessel with baffle. In the transition region Re_d is from 10 to 100, the isolated region as the term of “multiple isolated zones” were generated near the liquid free surface and the vessel bottom. The mixing pattern observed in rectangular vessel with any impeller, including the paddle, Rushton turbine, pitched paddle, and propeller impeller, can be predicted from the power correlation.

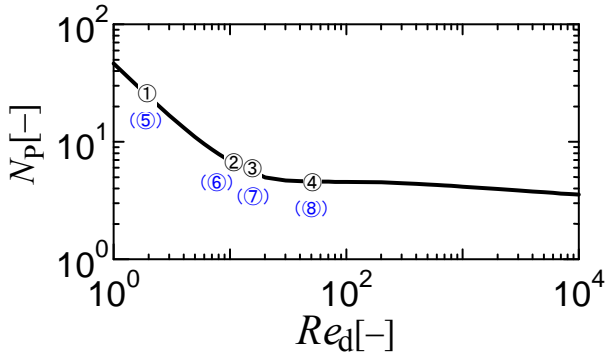


Fig. 3 Power number diagram for paddle impeller(1)

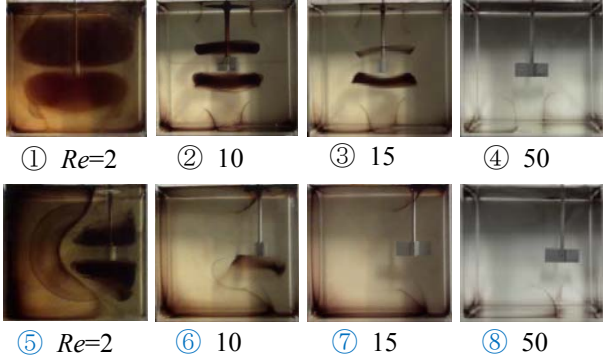


Fig. 4 Mixing patterns obtained with paddle impeller (1) in rectangular center mixing vessels ①-④ and in eccentric mixing vessels ⑤-⑧.

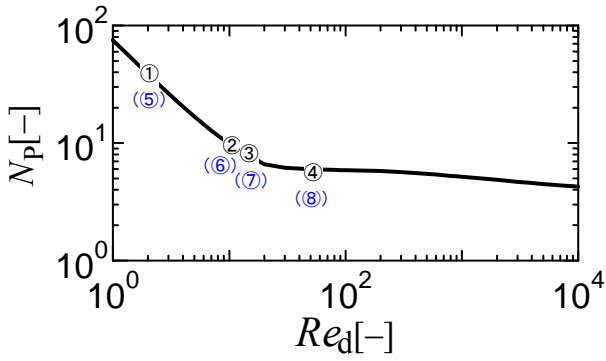


Fig. 5 Power number diagram for paddle impeller(2)

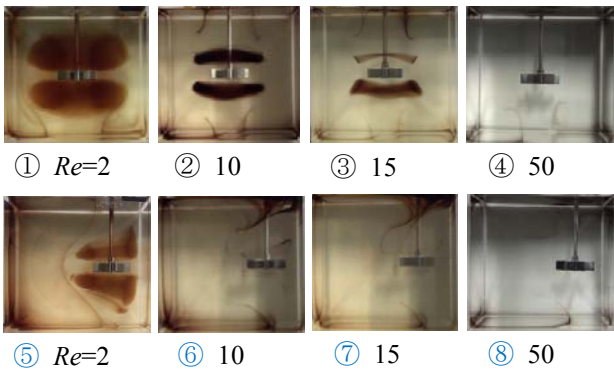


Fig. 6 Mixing patterns obtained with paddle impeller(2) in rectangular center mixing vessels ①-④ and in eccentric mixing vessels ⑤-⑧.

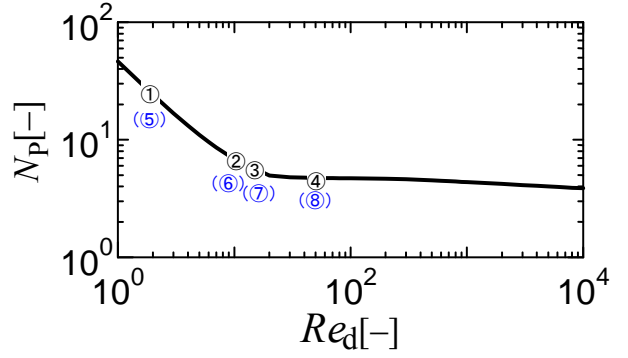


Fig. 7 Power number diagram for paddle impeller(1)

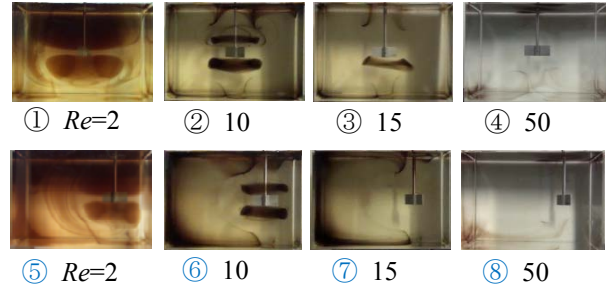


Fig. 8 Mixing patterns obtained with paddle impeller(1) in the larger rectangular vessel in center mixing vessels ①-④ and in eccentric mixing vessels ⑤-⑧.

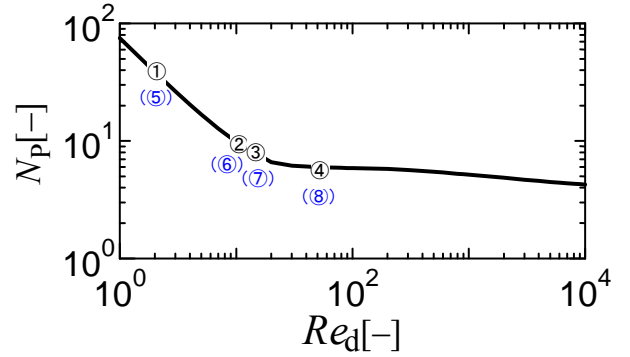


Fig. 9 Power number diagram for paddle impeller(2)

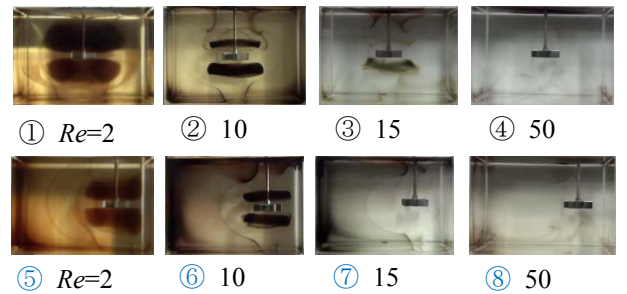


Fig. 10 Mixing patterns obtained with paddle impeller(2) in rectangular center mixing vessels ①-④ and in eccentric mixing vessels ⑤-⑧.

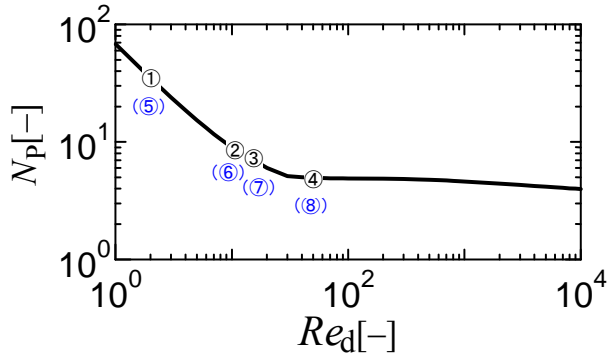


Fig. 11 Power number diagram for Rushton turbine(3)



Fig. 12 Mixing patterns obtained with Rushton turbine(3) in rectangular center mixing vessels ①-④ and in eccentric mixing vessels ⑤-⑧.

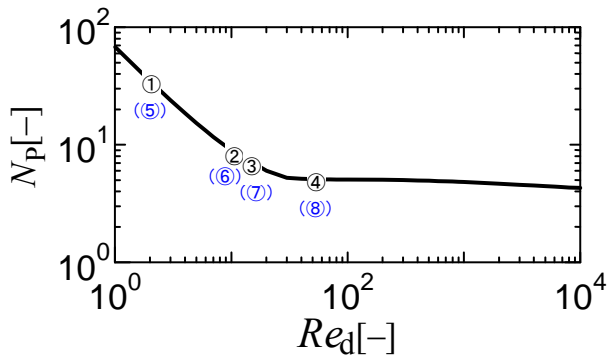


Fig. 13 Power number diagram for Rushton turbine(3)

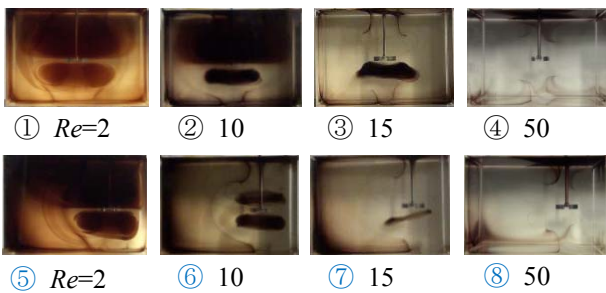


Fig. 14 Mixing patterns obtained with Rushton turbine (3) in larger rectangular center mixing vessels ①-④ and in eccentric mixing vessels ⑤-⑧.

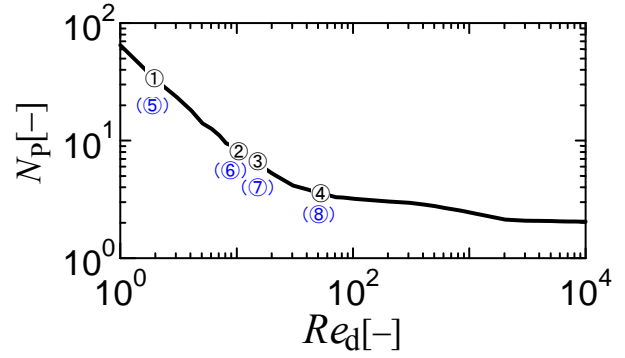


Fig. 15 Power number diagram for pitched paddle impeller(4)



Fig. 16 Mixing patterns obtained with pitched paddle impeller(4) in larger rectangular center mixing vessels ①-④ and in eccentric mixing vessels ⑤-⑧.

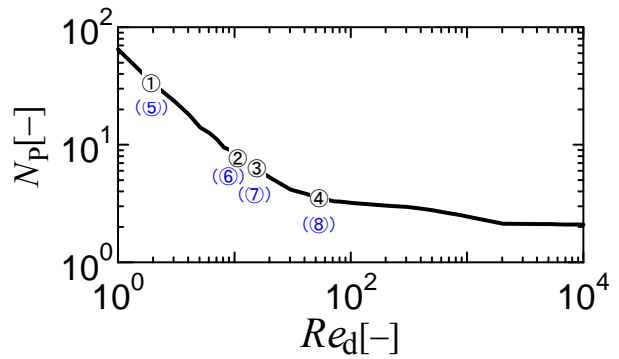


Fig. 17 Power number diagram for pitched paddle impeller(4)



Fig. 18 Mixing patterns obtained with pitched paddle impeller(4) in larger rectangular center mixing vessels ①-④ and in eccentric mixing vessels ⑤-⑧.

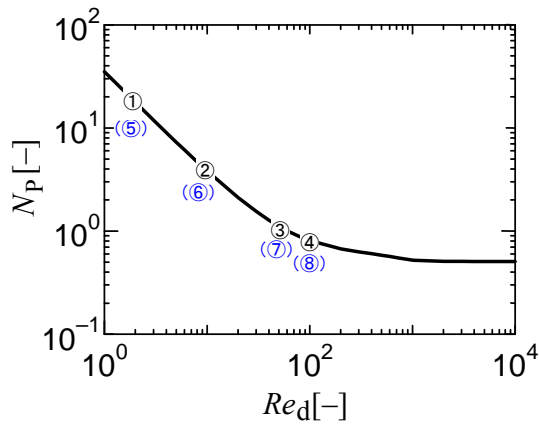


Fig. 19 Power number diagram for propeller impeller(5)

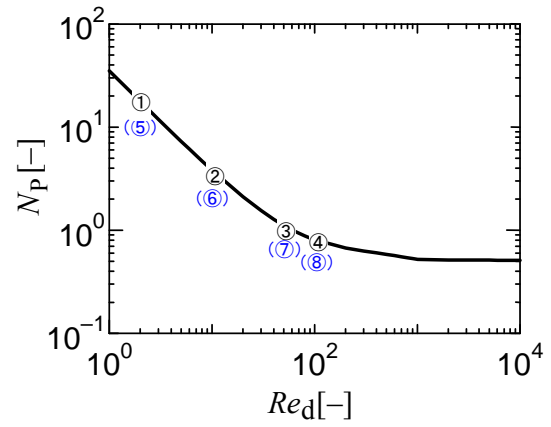


Fig. 21 Power number diagram for propeller impeller(5)



Fig. 20 Mixing patterns obtained with propeller impeller(5) in rectangular vessel in rectangular center mixing vessels ①-④ and in eccentric mixing vessels ⑤-⑧.

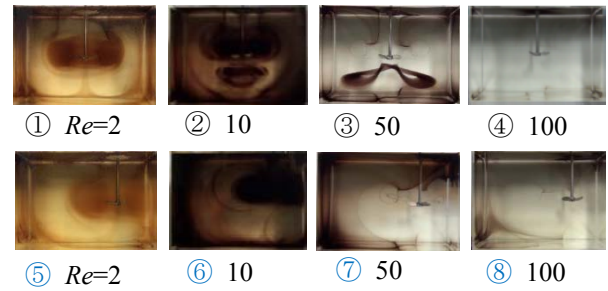


Fig. 22 Mixing patterns obtained with propeller impeller(5) in rectangular large vessel in rectangular center mixing vessels ①-④ and in eccentric mixing vessels ⑤-⑧.

Nomenclature

a	= short side of cross section for rectangular	[m]
a'	= long side of cross section for rectangular	[m]
b	= height of impeller blade	[m]
B_w	= baffle width	[m]
D	= characteristic length of diagonal for rectangular	[m]
d	= impeller diameter	[m]
H	= liquid depth	[m]
L_E	= eccentric length	[m]
N_p	= power number ($=P/\rho n^3 d^5$)	[-]
N_{p0}	= power number at non-baffled condition	[-]
N_{pmax}	= power number at fully baffled condition	[-]
n	= impeller rotational speed	[s ⁻¹]
n_B	= number of baffle plate	[-]
n_p	= number of impeller blade	[-]
P	= power consumption	[W]
Re_d	= impeller Reynolds number ($nd^2\rho/\mu$)	[-]
T	= shaft torque	[N · m]
t	= agitation operation time	[s]
θ	= angle of impeller blade	[-]
μ	= liquid viscosity	[Pa · s]
ρ	= liquid density	[kg · m ⁻³]

Literature Cited

- Furukawa H., Y. Kato, F. Kato, Y. Fukatsu and Y. Tada ; “Correlation of Power Consumption for Rectangular Mixing Vessel,” *Kagaku Kogaku Ronbunshu* , **39**,94—97(2013a)
- Furukawa H., Y. Kato, Y. Fukatsu and Y. Tada ; “Correlation of Power Consumption for Eccentric Rectangular Mixing Vessel with Propeller Impeller,” *Kagaku Kogaku Ronbunshu*, **39**,175—177(2013b)
- Furukawa H., Y. Kato, Y. Fukatsu Y. Tada, S. T. Koh and Y. S. Lee ; “Correlation of Power Consumption for an Eccentric Rectangular Mixing Vessel,” *Kagaku Kogaku Ronbunshu*, **39**, 479—484(2013c)
- Furukawa, H., Y. Kato, T. Kato and Y. Tada; “Power Correlations and Mixing Patterns of Several Large Paddle Impellers with Dished Bottom,” *J. Chem. Eng. Japan*, **46**, 255—261 (2013d)
- Kamei, N., S. Hiraoka, Y. Kato, Y. Tada, H. Shida, Y. S. Lee, T. Yamaguchi and S. T. Koh; “Power Correlation for Paddle Impellers in Spherical and Syindrical Agitated Vessels,” *Kagaku Kogaku Ronbunshu*, **21**, 41—48 (1995)
- Kamei, N., S. Hiraoka, Y. Kato, Y. Tada, K. Iwata, K. Murai, Y. S. Lee, T. Yamaguchi and S. T. Koh; “Effects of Impeller and Baffle Dimensions on Power Consumption under Turbulent Flow in an Agitated Vessel with Paddle Impeller,” *Kagaku Kogaku Ronbunshu*, **22**, 249—256 (1996)

- Kato, Y., Y. Tada, K. Urano, A. Nakaoka and Y. Nagatsu; “Differences of Mixing Power Consumption between Dished Bottom Vessel and Flat Bottom Vessel,” *Kagaku Kogaku Ronbunshu*, **36**, 25—29 (2010a)
- Kato Y., Y. Tada, Y. Takeda, N. Atsumi and Y. Nagatsui; “Prediction of Mixing Pattern from Power Number Diagram in Baffled and Unbaffled Mixing Vessels,” *J. Chem. Eng. Japan*, **43**, 46—51 (2010b)
- Nagata, S., T. Yokoyama and H. Maeda; “Studies on the Power Requirement of Paddle Agitators in Cylindrical Vessels,” *Kagaku Kogaku*, **20**, 582—592 (1956)
- Nishi, K., N. Enya, Y. Tanaka, R. Misumi and M. Kaminoyama; “Mixing in Eccentrically Located Hi-F Mixer,” *J. Chem. Eng. Japan*, **44**, 859—867 (2011)
- Takahashi, K., D. Shigihara and Y. Takahata; “Laminar Mixing in Eccentric Stirred Tank with Different Bottom,” *J. Chem. Eng. Japan*, **44**, 931-935 (2011)